

---

# Extending Pretrained 10-Second ECG Foundation Models to Longer Horizons

---

Wei Tang<sup>1</sup> Jinpei Han<sup>2</sup> Kangning Cui<sup>3</sup> Mattia Carletti<sup>6</sup> Fredrik K. Gustafsson<sup>6</sup>  
Shreyank N Gowda<sup>4</sup> Patitapaban Palo<sup>6</sup> Anshul Thakur<sup>6</sup> Lei Clifton<sup>6</sup>  
Jean-michel Morel<sup>5</sup> Raymond H. Chan<sup>5</sup> David A. Clifton<sup>6</sup> Xiao Gu<sup>6</sup>

<sup>1</sup>City University of Hong Kong <sup>2</sup>Imperial College London <sup>3</sup>Wake Forest University  
<sup>4</sup>University of Nottingham <sup>5</sup>Lingnan University <sup>6</sup>University of Oxford

## Abstract

Electrocardiogram (ECG) foundation models pretrained on typical diagnostic 10-second ECG segments, have demonstrated strong transferability across a range of clinical applications. However, many real-world applications produce recordings that are typically longer, and are varied in duration during inference time. These 10-second models have no built-in way to combine information across time. Extending them to longer horizons introduces two challenges: *structural* incompatibilities arising from input-length disparities, and *semantic* challenges that limit meaningful temporal aggregation. We propose a parameter-efficient framework that extends pretrained ECG foundation models to longer and variable-length ECGs without retraining the backbone. Guided by a frozen pretrained 10-second model, we introduce a lightweight plug-in module that extends the model in two complementary ways: (i) structurally compatible long-sequence processing and (ii) semantically informed temporal modeling. Experiments on multiple long-horizon ECG tasks, datasets, and foundation model backbones demonstrate that our method enables robust long-horizon extension from pretrained snapshot models, consistently outperforming sliding-window and pooling-based baselines with strong parameter efficiency.

## 1 Introduction

The electrocardiogram (ECG) remains the gold standard for non-invasive cardiovascular diagnosis, providing a direct view of cardiac electrical activity. Advances in machine learning, particularly deep neural networks, have substantially improved automated ECG analysis, with models achieving expert-level performance on several diagnostic tasks [1]. Early deep learning approaches, however, primarily relied on supervised training for narrow, task-specific objectives. While effective in controlled settings, these models were constrained by limited labeled data and often failed to generalize across datasets, institutions, and patient populations [2].

To improve robustness and transferability, recent work has increasingly shifted toward ECG foundation models pretrained with self-supervised objectives on large-scale ECG datasets [3–5]. Through contrastive or generative self-supervised learning objectives, these architectures learn generic feature extractors that are robust to signal variability and improve transfer across cohorts and institutions. As a result, a single pretrained foundation model backbone paired with lightweight task-specific heads can be adapted to diverse downstream applications such as diagnosis, phenotyping, and outcome prediction [6, 7].

Despite their progress, these ECG foundation models present a fundamental limitation: they are trained and used as fixed-length *snapshot* processors. They typically operate on short inputs (often

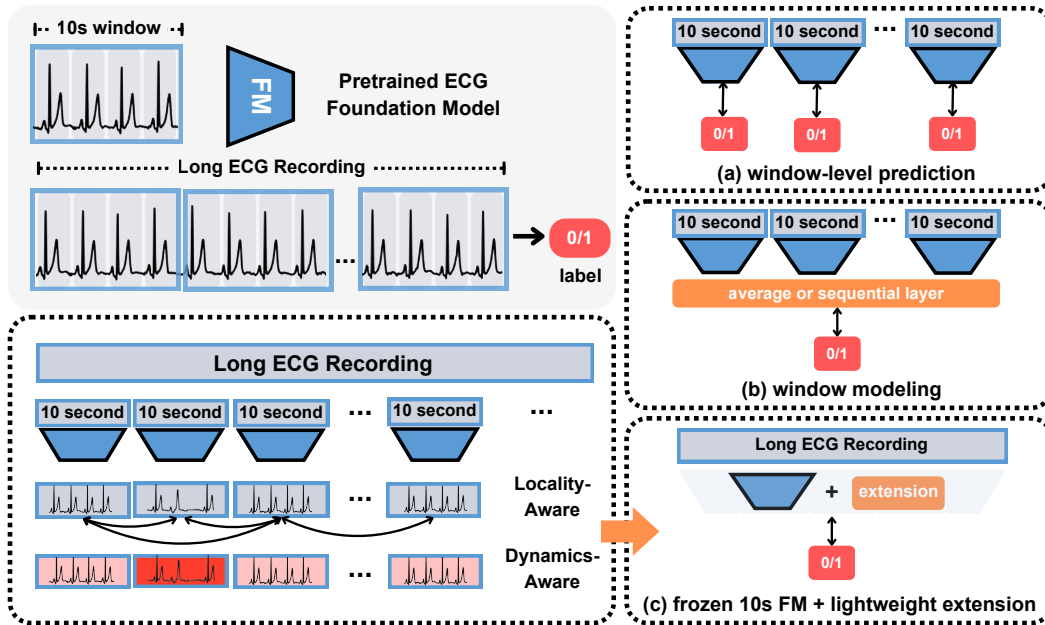


Figure 1: **Overview of the problem setting and extension strategies.** ECG foundation models are typically pretrained on short, fixed-length recordings (*e.g.*, 10 s), which makes direct use on long or variable-length recordings non-trivial. Naive extension strategies either run independent window-level predictions and aggregate the outputs as panel (a), or apply simple aggregation or sequential layers over window representations as panel (b). We propose a lightweight long-horizon extension for frozen 10-second ECG foundation models that supports variable-length longer recordings, by leveraging locality-aware inter-window similarity and dynamics-aware long-term learning, as illustrated in panel (c).

10 s) during both pretraining and inference [3, 4], which biases the learned representations toward local waveform morphology and short-term rhythm. As a result, they lack an explicit mechanism for aggregating information across extended recordings, modeling long-range temporal dependencies, or supporting coherent prediction across multiple horizons – when recording duration varies across monitoring scenarios.

This limitation is consequential for many clinically relevant settings. In contrast to short 12-lead diagnostic recordings, continuous monitoring is intended to capture sparse or intermittent events over longer horizons, often under reduced-lead configurations [8–10]. In these contexts, clinically actionable signals may be distributed unevenly over time, as in paroxysmal atrial fibrillation surveillance, sleep, or sepsis early-warning. A common workaround is sliding-window inference followed by simple aggregation (*e.g.*, mean pooling) of window-level outputs (Figure 1a). More structured variants aggregate window representations using attention or lightweight sequential modules (Figure 1b). While practical, such strategies can be computationally costly and still model cross-window dependencies only indirectly, motivating adaptation methods that explicitly extend the model temporal horizon beyond the original snapshot setting.

In this work, we show that pretrained snapshot ECG foundation models can be adapted to longer-duration and variable-length inputs without computationally expensive retraining. Our key observation is that these models can be repurposed for extended-context ECG analysis along three complementary dimensions, as illustrated in Figure 1 (left bottom panel).

**General ECG interpretation.** Pretrained ECG foundation models already acquire substantial domain knowledge for interpreting cardiac signals through large-scale pretraining. This enables knowledge to be preserved and effectively reused when extending the models to longer temporal horizons, without relearning low-level ECG semantics.

**Locality-aware representation learning.** Pretrained ECG foundation models are already well suited to encode short 10-second ECG windows: each segment can be meaningfully represented on its own, thus can be used as a local reference when extending the model to longer recordings. We exploit this property to preserve local semantics and align snapshot-level representations when processing long recordings.

**Dynamics-aware long-term learning.** The representations produced by pretrained models naturally reflect relative importance across segments, offering a basis for identifying informative events within long recordings. This property allows selective reuse and robust aggregation of local representations, which is essential for modeling sparse and transient dynamics over extended time horizons.

Based on these insights, we propose a parameter-efficient framework that extends frozen snapshot ECG foundation model to longer-horizon and variable-length settings. Rather than modifying or retraining the pretrained backbone, we reuse its embedded ECG knowledge and locality prior, while introducing a lightweight module to explicitly model long-term temporal dynamics. Across diverse datasets, tasks, and models, our method consistently improves long-horizon performance over conventional sliding-window and pooling strategies, demonstrating a practical and scalable path that goes beyond 10-second ECG understanding.

## 2 Related Work

**ECG foundation models.** Foundation models have recently been extended from vision and language to physiological signals, with ECG serving as a prominent testbed. Most existing ECG foundation models are pretrained on diagnostic ECG recordings, which are typically short in duration ( $\approx 10$  s) and acquired using standard 12-lead configurations [3, 4]. To date, most progress in this field has been driven along two complementary dimensions: scaling the volume and diversity of pretraining data [6, 7, 11, 12], and refining pretraining strategies to better exploit available supervision (self-supervised [13], hybrid [14], or knowledge-informed objectives [15, 16]). On the other hand, these models, pretrained in a diagnostic 10-second 12-lead regime, have been shown to generalize seamlessly to reduced-lead or single-lead settings [6, 7], which are widely used in continuous monitoring scenarios. However, they remain fundamentally limited in their ability to operate directly over longer temporal horizons, in an end-to-end manner, beyond simplistic sliding-window processing of 10 s segments.

**Long-term physiology modeling.** Many clinically relevant decisions depend on physiological dynamics over long horizons, which are not well captured by short snapshot windows, such as ambulatory Holter monitoring and intensive care monitoring. Recent learning-based systems often apply window slicing, which partitions a long recording into short segments, produces segment-level predictions or embeddings, and then aggregates these across time. The aggregation strategy varies from simple pooling to the more recent attention pooling or a lightweight sequential layer like LSTM to model the temporal relationships [17, 18]. However, such aggregation introduces a structural bottleneck: As most tasks are formulated as mapping a single long sequence to a single outcome, temporal dependencies within the sequence are often weakly modeled, making it difficult to localize when clinically meaningful risk signals occur. Moreover, performance can degrade when predictions are made from observations that are shorter than the horizon assumed by the aggregation, limiting utility in time-sensitive clinical decision-making.

**Adaptation of biosignal foundation models.** Alongside the emergence of ECG foundation models, or broader biosignal foundation models, increasing attention has been paid to adaptation under distribution shifts [19] and deployment constraints [20]. They are mostly enabled by parameter-efficient fine-tuning methods such as LoRA, prefix tuning, and adapter modules, which update only a small subset of parameters while largely preserving the backbone [21]. Despite this progress, existing biosignal adaptation work primarily targets task transfer, domain shift, and personalization under a fixed input scale. It assumes that the downstream signal can be processed within the same short window length used in pretraining. Due to the nature of most existing ECG datasets, which were typically collected in standard diagnostic settings (often 10 s), the models pretrained on these datasets fall short when applied to longer temporal horizons required in several clinical settings. A systematic approach to extend the temporal horizon of pre-trained biosignal foundation models during adaptation remains unexplored.

## 3 Method

We focus on ECG foundation models based on transformer architectures and denote by  $f_\theta$  the backbone foundation model, parameterized by  $\theta$ , whose parameters are kept frozen. The input to the backbone model is an ECG signal, processed as a sequence of fixed-length patch-level embeddings (e.g., 0.1 s), which are augmented with positional embeddings to encode temporal order before being passed to the transformer. Specifically, the ECG input embedding is denoted as  $\mathbf{X} \in \mathbb{R}^{N_{[10s]} \times D}$ ,

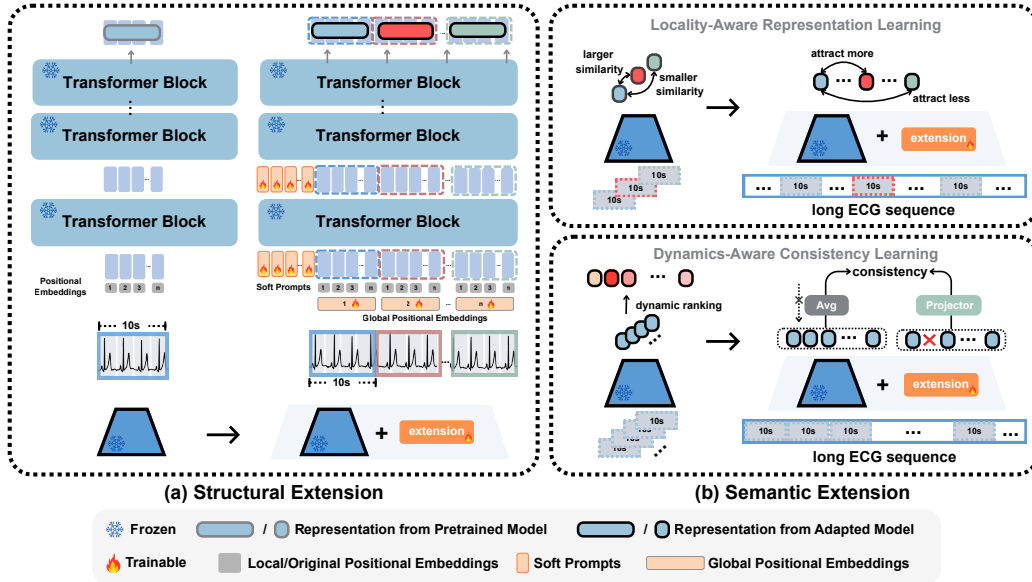


Figure 2: **Overview of our extension framework.** The extension is divided into two complementary parts: a structural extension that enables compatibility with long-horizon recordings, and a semantic extension that supports coherent representation learning over extended temporal horizons. (a) Structural extension (Section 3.1) introduces additional learnable tokens, soft prompts and global positional embeddings, by freezing the original backbone model, to make it compatible with longer recordings. (b) Semantic extension (Section 3.2) leverages snapshot-level (10-second) representations derived from the frozen backbone as supervision, enforcing semantic consistency across segments and supporting coherent long-horizon understanding.

where  $N_{[10s]}$  is the number of patches and  $D$  is the embedding dimension. The corresponding positional embeddings  $\mathbf{E}_{[10s]} \in \mathbb{R}^{N_{[10s]} \times D}$ , are added to  $\mathbf{X}$  and passed to the backbone model  $f_\theta$  to produce a global representation of the signal,  $f_\theta(\mathbf{X} + \mathbf{E}_{[10s]})$ . Existing ECG foundation models are typically pretrained on short, fixed-length segments (*e.g.*, 10-second windows) and achieve strong performance by learning generalizable representations of local waveform morphology and short-term rhythm. However, applying these models directly to longer horizons poses two fundamental challenges.

- **Structural extension.** At a structural level, snapshot ECG models are not directly compatible with longer recordings. Their positional encodings, tokenization schemes, and input assumptions are optimized for short segments.
- **Semantic extension.** Beyond input compatibility, long-horizon ECG analysis requires meaningful aggregation of information across time. Clinically relevant events may be sparse, transient, or distributed unevenly over long recordings. Naively processing each 10-second segment independently and pooling predictions fails to capture long-range dependencies.

These two challenges motivate a framework that not only enables snapshot ECG foundation models to operate on long recordings, but also extends their semantic understanding to support coherent long-term modeling. To this end, we propose a framework, illustrated in Figure 2, that performs a single adaptation to long-horizon ECG signals ( $\mathbf{X} \in \mathbb{R}^{N_{[L]} \times D}$ , with  $L > 10$  s) and supports inference across variable signal lengths up to  $L$  without further modification. The empirical value for  $L$  considered in the main experiments is 180 s.

### 3.1 Structural Extension - Enabling Long-Horizon ECG Processing

A critical barrier to adapting snapshot models to extended recordings lies in the incompatibility of positional embeddings. These embeddings  $\mathbf{E}_{[10s]} \in \mathbb{R}^{N_{[10s]} \times D}$  are learned for a fixed input length and therefore encode temporal relationships that are specific to a 10-second window.

In the image domain, a common practice for extending vision transformers to different image scales [22–24], is interpolating positional embeddings. However, this strategy does not naturally transfer to

time series, especially biosignals, since interpolation has fundamentally different meanings between these two domains. The former (image) is related to resolutions, whilst the latter (biosignal) is related to the sampling rate, which is significantly entangled with their physiological information.

To address this, rather than interpolating from  $N_{[10s]}$  to  $N_{[L]}$ , we introduce a two-level positional encoding scheme, comprising local (fine-grained, the original  $\mathbf{E}_{[10s]}$ ) and global (coarse-grained,  $\mathbf{E}_{\text{global}}$ ) components. The former reuses the original  $\mathbf{E}_{[10s]}$  to preserve within-10-second temporal structure, whereas the latter models the relationship between consecutive 10-second segments. For a sequence of  $N_{[L]}$  patches, we construct the final positional embedding  $\mathbf{E}_{[L]} \in \mathbb{R}^{N_{[L]} \times D}$  as:

$$\mathbf{E}_{[L]}[t] = \mathbf{E}_{[10s]}[t \bmod N_{[10s]}] + \mathbf{E}_{\text{global}}[\lfloor t/N_{[10s]} \rfloor], \quad (1)$$

where  $t$  indexes the patch and  $\lfloor t/N_{[10s]} \rfloor$  indexes its associated 10-second segment for global temporal encoding.

**Local component ( $\mathbf{E}_{[10s]}$ ).** This component inherits the pre-trained positional weights, preserving sensitivity to high-frequency intra-segment structures (*e.g.*, P-QRS-T complexes). For sequences exceeding the pretraining length, we repeat these weights rather than interpolating them, preserving the temporal scale at which local waveform morphology was learned during pretraining.

**Global component ( $\mathbf{E}_{\text{global}}$ ).** To anchor local windows within the broader recording context, we introduce a learnable embedding matrix  $\mathbf{E}_{\text{global}} \in \mathbb{R}^{M \times D}$ , where  $M = N_{[L]}/N_{[10s]}$  denotes the number of 10-second segments in the signal. For simplicity and without loss of generality, we assume that  $N_{[L]}$  is an integer multiple of  $N_{[10s]}$ . Each embedding in  $\mathbf{E}_{\text{global}}$  is then broadcast across a contiguous block of  $N_{[10s]}$  patches by Equation 1.

This hierarchical design enables modeling over the full recording duration while maintaining the frequency characteristics and morphological semantics learned within local segments during pretraining.

**Soft prompt tuning.** To facilitate the learning of global positional embeddings and enable parameter-efficient adaptation to capture long-horizon temporal relationships, we adopt soft prompt tuning by introducing additional learnable tokens that are prepended to the input sequence and inserted at intermediate layers [25].

### 3.2 Semantic Extension - Extending Long-Horizon ECG Understanding

A purely structural extension to longer signals does not, by itself, work directly on longer signals, as the additional components introduced by the extension are randomly initialized. Directly and solely optimizing learnable components in an end-to-end manner, by mapping the long-sequence to a single label, may result in suboptimal extension and may be insufficient for effective long-range modeling.

To address this, we take the hypothesis that the backbone foundation model  $f_\theta$  itself already learns representations that are sufficiently informative at any 10-second scale locally, and when applied to consecutive 10-second segments, can be leveraged to capture dynamics over longer horizons. In this sense, we adopt a teacher-student framework, where the representation derived from each 10-second segment serves as the teacher to guide the representation learning both locally and globally over extended temporal horizons.

**Locality-aware representation learning.** We first enforce segment-level semantic alignment between the pretrained and extended models. The pretrained foundation model is trained on short (10-second) ECG segments and provides robust local representations of morphology, rhythm, and physiological state. When adapting the model to longer ECG sequences, these local representations may be changed by the long-horizon training objective. To reduce this risk, we constrain the student model to remain aligned with the pretrained teacher at the segment level.

We implement this using teacher-guided soft contrastive learning. Prior approaches define contrastive pairs based on temporal adjacency [26] or patient identity [27]. In contrast, we compute soft similarity targets from teacher-derived representations within each batch, thereby preserving the teacher-induced similarity structure without imposing explicit temporal or patient-level pairing assumptions.

We use pairwise similarities between teacher representations as soft supervision to guide the student via a contrastive objective. Let  $\mathbf{S}_{i,j}^T$  denote the similarity (*e.g.*, negative  $L_2$  norm) between teacher representations of local 10-s segments  $i$  and  $j$ . For an anchor segment  $i$ , if  $\mathbf{S}_{i,j}^T > \mathbf{S}_{i,k}^T$ , the student is encouraged to preserve the same ordering, *i.e.*,  $\mathbf{S}_{i,j}^S > \mathbf{S}_{i,k}^S$ . This is implemented using a rank-

based soft contrastive loss [28], which preserves the relative ranking of inter-segment similarities. Figure 2 (right upper panel) illustrates this similarity-based alignment, with the local contrastive loss formulated as below:

$$\mathcal{L}_{\text{local}} = -\frac{1}{K} \sum_{\substack{j=1 \\ j \neq i}}^K \log \frac{\exp(\mathbf{S}_{i,j}^S/\tau)}{\sum_{k \in \Omega_{i,j}} \exp(\mathbf{S}_{i,k}^S/\tau) + \exp(\mathbf{S}_{i,j}^S/\tau)}, \quad (2)$$

where  $K$  denotes the number of segments in the batch, and  $\tau$  is a temperature parameter. The set  $\Omega_{i,j}$  is defined based on the teacher similarity as  $\Omega_{i,j} = \{k \mid \mathbf{S}_{i,k}^T < \mathbf{S}_{i,j}^T\}$ , *i.e.*, all segments that are ranked as less similar to anchor  $i$  than segment  $j$  according to the teacher. In practice, we add a projector  $g_{\text{local}}(\cdot)$  on top of the latent representation to implement this loss, following standard practice in contrastive learning [29].

**Dynamics-aware consistency learning.** Physiological signals such as ECG are inherently non-stationary, exhibiting pronounced temporal variability over long recordings. Rather than assuming that all 10-second segments should contribute in the same way, we use the frozen teacher representation to partition segments according to their similarity structure. This partition is used as an operational mechanism for organizing heterogeneous segments (such as rare abnormal events versus stationary patterns, or clean versus less clean segments), and empirically, we found that using both groups consistently outperforms using either group alone, which indicates that both high-variation and lower-variation parts contain useful information. We therefore encourage each group to retain information from the whole recording, to capture global dynamics.

To implement this idea, we identify a subset of 10-second segments  $\mathcal{I}_{bg}$  that are most consistent with the rest of the recording, using an affinity matrix computed by the frozen teacher encoder. Intuitively, the affinity matrix encodes the pairwise similarity between all segments, and high-affinity (ha) segments  $\mathcal{I}_{ha}$  are selected by ranking across the affinity matrix. We then encourage these high-affinity segments to remain aligned to the global representations, remaining as consistent as possible even when the more dynamic segments are excluded. Specifically, the consistency is achieved as below:

$$\mathcal{L}_{\text{dyn}} = \frac{1}{|\mathcal{I}_{ha}|} \sum_{i \in \mathcal{I}_{ha}} \mathcal{D}_{\text{cos}} \left( g_{\text{dyn}}(\mathbf{z}_S^{(i)}), \text{stopgrad}(\bar{\mathbf{z}}_S) \right), \quad (3)$$

where  $\mathbf{z}_S^{(i)}$  denotes the student feature for 10-second segment  $i$ ,  $\bar{\mathbf{z}}_S$  is the global feature by averaging latent features over the entire long-horizon sequence, and  $\mathcal{D}_{\text{cos}}$  is the cosine distance. In practice, we apply a one-sided  $g_{\text{dyn}}(\cdot)$  projection head to the student representations, and a stop-gradient  $\text{stopgrad}(\cdot)$  operator through global representation, to prevent trivial collapse to constant representations [30].

### 3.3 Model Training

We train the framework end-to-end by minimizing:

$$\mathcal{L} = \mathcal{L}_{\text{task}} + \lambda_1 \mathcal{L}_{\text{local}} + \lambda_2 \mathcal{L}_{\text{dyn}}, \quad (4)$$

where  $\mathcal{L}_{\text{task}}$  is the standard classification loss,  $\lambda_1$  and  $\lambda_2$  are scalar weighting coefficients that balance the contribution of each auxiliary loss.

## 4 Experiments

We evaluate the proposed framework on four downstream task settings and four foundation model backbones. This setup allows us to assess long-horizon adaptation across diverse clinical scenarios, model scales, and pretraining paradigms.

**Evaluation setup.** Unless otherwise specified, all models are trained on 3-minute ECG recordings and evaluated on 3-minute, 2-minute, 1-minute, 30-second, and 10-second inputs without retraining. This protocol reflects realistic deployment settings in which the available monitoring duration may vary [31], while keeping the focus on practical extension beyond the original 10-second duration.

**Backbone models.** We use four backbone configurations from three representative ECG foundation-model families: CSFM [6] (Tiny and Base), MERL [32], and ECG-JEPA [33]. These backbones vary in model scale and pretraining objective, providing a diverse test bed for evaluating the robustness and generality of the proposed framework.

## 4.1 Datasets & Tasks

We consider three datasets covering four downstream task settings in total. All datasets are preprocessed using a standardized pipeline before training and evaluation.

**VTaC** [8, 34] is a critical care benchmark for reducing false ventricular tachycardia (VT) alarms. We use the final 3 minutes preceding the alarm onset and formulate the task as binary classification of true versus false VT alarms.

**MC-MED** [10, 35] contains emergency department records and is used for two prediction tasks: *ED disposition* prediction, formulated as binary classification of *Discharge* versus *Admission*, and *triage acuity* prediction, formulated as five-class classification. For both tasks, we use the lead-II ECG signal and extract the final 3 minutes of the selected segment.

**CPSC2021** [36] is a long-term Holter benchmark targeting paroxysmal atrial fibrillation (AF) events. We formulate it as a binary AF detection task using the lead-II signal and segment long recordings into non-overlapping 3-minute windows.

## 4.2 Baseline Methods

We compare the proposed method with two groups of baseline strategies: *Snapshot Aggregation* includes Token Pooling and Logit Pooling. These methods partition each long ECG into non-overlapping 10-second windows and aggregate either frozen backbone features or window-level logits. *Fine-tuning-based Adaptation* includes Full Fine-tuning, Linear Probing, Partial Tuning, Bias Tuning, Adapter, Visual Prompt Tuning (VPT) [25, 37, 38], and an LSTM-based baseline. These methods adapt either the pretrained model parameters or the resulting sequence of snapshot features for longer recordings. For baselines that require longer inputs, positional embeddings are extended by interpolation.

## 5 Results

**Main Results on Long-Horizon ECG Tasks.** Table 1 summarizes the adaptation results across four backbone configurations and four downstream task settings. For each task, we report both performance at 3-minute and the average across all evaluated inference durations (3-minute, 2-minute, 1-minute, 30-second, and 10-second). Overall, the proposed method is consistently among the strongest approaches across tasks and backbones, and in most cases outperforms both snapshot aggregation baselines and lightweight adaptation methods.

A clear pattern also emerges across methods. Snapshot aggregation strategies such as logit pooling and token pooling provide competitive baselines in several settings, but they are typically outperformed in longer temporal context across tasks and backbones. This suggests that simple aggregation over short-window predictions or features is often insufficient for robust long-horizon adaptation.

The backbone-specific trends are also informative. On the CSFM family and ECG-JEPA, the proposed method achieves the strongest overall performance in most settings, particularly at longer input durations. On MERL, full fine-tuning remains the strongest baseline overall, whereas the proposed method remains highly competitive and often achieves the second-best performance while keeping the pretrained backbone frozen. Taken together, these results indicate that the proposed framework provides a reliable way to extend snapshot ECG foundation models across tasks, backbone scales, and pretraining paradigms.

**Guidance Source Analysis.** The MERL results motivate a more focused question: how much does semantic extension depend on the quality of the teacher representation? On VTaC, MERL self-guidance is noticeably weaker than full fine-tuning, and snapshot aggregation baselines are also relatively poor. This suggests that the snapshot-level MERL representations may provide a less effective guidance signal for long-horizon extension in this setting.

To examine this effect, we replace MERL self-guidance with external guidance from stronger backbone models while keeping the MERL student unchanged. As shown in Table 2, all three external guidance sources consistently improve over MERL self-guidance across inference durations, with the gains becoming more pronounced beyond 30 s. Figure 3 further provides qualitative evidence that the different backbones induce different feature-space structures on VTaC, which is consistent

Table 1: **Main adaptation results across ECG foundation models and downstream tasks.** For each task, we report performance at the longest evaluation horizon (180s) together with the average across five input lengths in the format **Avg. (Std.)**. **Best** results are shown in bold and second-best results are underlined.

Method	VTaC		MC-MED (ED)		MC-MED (Acuity)		CPSC2021		Overall Avg.
	180s	Avg. (Std.)	180s	Avg. (Std.)	180s	Avg. (Std.)	180s	Avg. (Std.)	
<i>CSFM-Tiny</i>									
Token Pooling	74.05	76.24 (2.28)	70.80	68.72 (2.69)	61.00	60.00 (1.03)	96.81	96.59 (0.39)	75.39
Logit Pooling	73.83	75.83 (1.96)	71.15	<u>69.28</u> (2.26)	60.13	59.96 (0.48)	97.23	97.26 (0.16)	75.58
Full Fine-tuning	79.01	70.54 (6.89)	70.81	68.09 (3.05)	<b>64.80</b>	<u>63.07</u> (1.18)	94.24	93.23 (1.91)	73.73
Linear Probing	69.50	71.10 (1.25)	69.38	66.89 (2.67)	60.66	60.08 (0.99)	96.46	96.91 (0.57)	73.75
Partial Tuning	86.49	73.57 (9.59)	70.91	68.47 (3.79)	63.43	63.06 (1.50)	95.48	94.87 (1.57)	74.99
Bias Tuning	64.43	66.43 (1.94)	68.13	66.28 (1.93)	56.71	54.49 (2.42)	98.46	97.62 (1.33)	71.21
Adapter	79.33	72.83 (5.08)	71.24	68.60 (3.01)	61.55	60.53 (0.94)	98.01	96.24 (2.99)	74.55
VPT	<u>88.18</u>	74.33 (10.78)	71.19	67.29 (5.16)	64.50	61.22 (3.17)	98.67	96.37 (3.94)	74.80
LSTM Tuning	84.97	<u>83.01</u> (2.39)	<u>71.31</u>	65.18 (7.55)	61.97	58.80 (4.55)	<u>98.75</u>	<u>98.09</u> (0.63)	<u>76.27</u>
<b>Ours</b>	<b>89.50</b>	<b>88.13</b> (2.32)	<b>72.02</b>	<b>69.79</b> (3.18)	<b>65.18</b>	<b>63.35</b> (2.04)	<b>98.86</b>	<b>98.63</b> (0.79)	<b>79.98</b>
<i>CSFM-Base</i>									
Token Pooling	77.94	79.84 (2.09)	71.23	69.30 (2.51)	66.82	64.76 (2.36)	97.02	97.33 (0.40)	77.81
Logit Pooling	77.83	79.64 (1.98)	71.59	<u>69.90</u> (2.46)	67.07	64.85 (2.46)	97.54	97.52 (0.23)	77.98
Full Fine-tuning	84.23	72.46 (9.58)	72.30	69.83 (3.13)	65.09	63.47 (1.46)	95.66	95.66 (1.13)	75.35
Linear Probing	74.35	77.50 (2.81)	70.44	67.86 (2.64)	66.53	64.26 (2.32)	96.89	96.86 (0.25)	76.62
Partial Tuning	88.81	79.69 (8.23)	71.47	69.29 (3.41)	67.25	65.06 (2.11)	96.21	95.54 (1.00)	77.40
Bias Tuning	70.35	73.35 (2.02)	71.36	68.87 (3.16)	60.66	58.90 (1.77)	98.39	97.23 (1.39)	74.59
Adapter	88.43	78.95 (7.96)	71.90	69.22 (3.45)	65.91	63.72 (2.00)	98.41	96.85 (2.87)	77.19
VPT	<u>90.24</u>	80.72 (7.93)	<u>72.39</u>	68.76 (5.25)	66.00	63.78 (3.03)	98.57	96.57 (2.89)	77.46
LSTM Tuning	86.93	<u>85.22</u> (1.33)	72.03	67.77 (6.33)	68.14	<u>65.18</u> (2.95)	98.74	98.31 (0.47)	79.12
<b>Ours</b>	<b>91.23</b>	<b>89.62</b> (1.53)	<b>72.89</b>	<b>70.36</b> (3.43)	<b>68.89</b>	<b>66.00</b> (2.65)	<b>99.56</b>	<b>98.46</b> (1.08)	<b>81.11</b>
<i>ECG-JEPA</i>									
Token Pooling	76.76	78.54 (1.56)	69.75	67.37 (2.74)	61.38	60.33 (1.30)	90.75	90.68 (0.55)	74.23
Logit Pooling	76.23	78.10 (1.65)	69.23	67.67 (2.46)	61.23	60.11 (1.28)	90.14	90.47 (0.57)	74.09
Full Fine-tuning	88.32	82.96 (5.44)	67.96	65.44 (2.27)	62.83	60.65 (1.56)	88.67	89.59 (0.83)	74.66
Linear Probing	77.21	79.00 (1.45)	70.32	66.49 (3.04)	63.71	61.90 (1.46)	88.83	89.33 (0.34)	74.18
Partial Tuning	88.89	<u>84.32</u> (5.27)	70.19	67.79 (2.92)	64.59	62.54 (2.20)	88.33	89.05 (0.76)	75.93
Bias Tuning	86.83	83.68 (5.53)	<u>72.14</u>	<u>69.53</u> (2.77)	65.50	<u>64.06</u> (1.62)	85.41	84.86 (2.20)	75.53
Adapter	70.57	67.91 (2.44)	63.06	60.68 (2.34)	60.77	60.17 (0.60)	75.88	73.17 (4.10)	65.48
VPT	89.87	82.44 (7.97)	<b>72.48</b>	67.29 (6.11)	<u>66.18</u>	63.89 (3.53)	<u>93.65</u>	84.85 (10.15)	74.62
LSTM Tuning	85.17	82.66 (2.67)	70.72	68.39 (3.15)	65.18	62.93 (2.35)	91.26	<u>90.90</u> (0.49)	<u>76.22</u>
<b>Ours</b>	<b>91.02</b>	<b>85.65</b> (4.91)	<b>72.48</b>	<b>70.69</b> (3.35)	<b>67.53</b>	<b>64.89</b> (2.63)	<b>94.66</b>	<b>90.92</b> (4.25)	<b>78.04</b>
<i>MERL</i>									
Token Pooling	71.56	69.47 (3.97)	68.79	65.49 (3.85)	66.82	64.76 (2.36)	88.31	86.59 (3.38)	71.58
Logit Pooling	71.37	69.32 (3.88)	68.81	65.47 (3.78)	67.07	64.85 (2.46)	86.56	85.79 (2.59)	71.36
Full Fine-tuning	<b>88.31</b>	<b>82.08</b> (7.39)	67.30	65.03 (2.81)	65.09	63.47 (1.46)	<b>95.72</b>	<b>91.50</b> (7.41)	<b>75.52</b>
Linear Probing	74.91	71.94 (3.98)	68.07	64.64 (5.25)	66.53	64.26 (2.32)	84.52	82.86 (2.40)	70.93
Partial Tuning	79.06	71.59 (6.79)	68.41	64.98 (4.60)	67.25	65.06 (2.11)	88.71	87.32 (2.78)	72.24
Bias Tuning	80.63	75.62 (6.72)	69.12	<u>65.57</u> (4.52)	60.66	58.90 (1.77)	94.10	88.26 (6.51)	72.09
Adapter	74.72	71.16 (4.38)	68.36	65.39 (4.77)	65.91	63.72 (2.00)	89.39	88.52 (2.24)	72.20
VPT	80.74	71.94 (8.67)	<u>69.74</u>	64.29 (5.69)	66.00	63.78 (3.03)	91.75	85.59 (8.69)	71.40
LSTM Tuning	<u>83.05</u>	<u>78.55</u> (5.44)	67.74	63.86 (3.97)	68.14	<u>65.18</u> (2.95)	93.55	89.01 (5.96)	74.15
<b>Ours</b>	82.60	76.76 (9.16)	<b>69.92</b>	<b>65.76</b> (5.32)	<b>68.89</b>	<b>66.00</b> (2.65)	93.49	<u>89.73</u> (5.89)	<u>74.56</u>

with their different effectiveness as guidance sources. Together, these results suggest that long-horizon semantic extension depends, at least in part, on the informativeness of the underlying snapshot-level teacher representation.

**Modality-Agnostic Analysis.** The long-horizon extension problem is not unique to ECG. Other physiological signals are also commonly modeled using short snapshot windows despite containing clinically meaningful information over longer durations. To test whether the proposed framework generalizes beyond ECG-only inputs, we evaluate CSFM-Tiny on VTaC using ECG-only, PPG-only, and joint ECG+PPG settings. Figure 4 shows that our method consistently outperforms the baseline adaptation strategies across all three modality configurations. This result suggests that the proposed framework is not tied to a single physiological modality, but instead addresses a broader limitation of snapshot-pretrained physiological models.

**Ablation Study.** We next examine which components of the proposed framework drive its gains. Table 3 isolates the effects of the positional encoding strategy, locality-aware learning, and dynamics-aware consistency learning on VTaC using CSFM. Replacing repeated or interpolated positional encodings with the proposed global positional encoding already yields a clear improvement, indicating that structural compatibility with longer recordings is an important component of long-horizon

Table 2: **Guidance source comparison for MERL on VTaC.** Results are reported as AUC (%) across different inference durations.

Guidance	10s	30s	60s	120s	180s
MERL Self-guided	61.23	76.03	80.27	83.68	82.60
CSFM-Tiny guided	62.67	79.64	83.46	84.64	85.19
CSFM-Base guided	<b>63.16</b>	<b>81.33</b>	<b>84.51</b>	84.99	<b>86.07</b>
ECG-JEPA guided	63.07	80.61	84.17	<b>85.03</b>	85.78

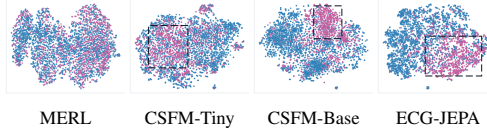


Figure 3: **t-SNE visualizations of feature space on VTaC.** Blue and purple denote different classes. The dashed boxes highlight regions with clearer class separation, indicating stronger teacher model.

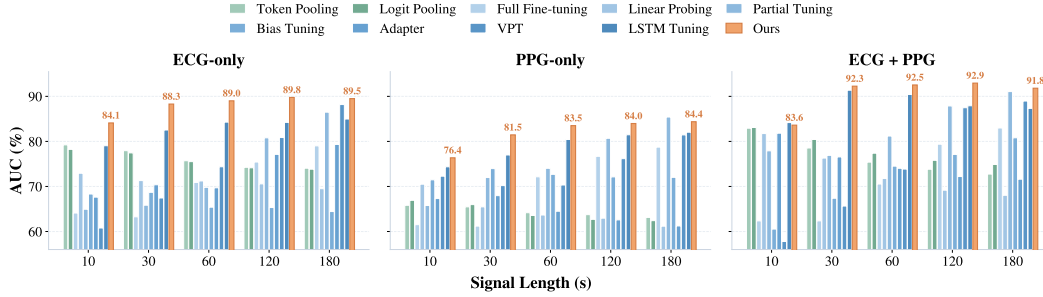


Figure 4: **Generalization across signal modalities on VTaC.** We evaluate the proposed framework using CSFM-Tiny under ECG-only, PPG-only, and joint ECG+PPG settings. Across all three modality configurations, the proposed method consistently outperforms the baseline adaptation strategies, indicating that the long-horizon extension is not specific to ECG alone.

extension. Adding either the locality-aware objective or the dynamics-aware objective provides further gains, while combining both produces the strongest overall performance across input durations.

**Affinity-guided dropping.** We further analyze the consistency module through affinity-guided segment dropping. Compared with random dropping, affinity-guided dropping is generally more effective, supporting the role of similarity-based segment structure in the dynamics-aware objective. Taken together, these ablations show that the gains of the proposed framework arise not from simple input resizing or generic tuning alone, but from the combination of structural extension and semantically informed temporal adaptation.

## 6 Conclusion

In this work, we studied how to extend snapshot ECG foundation models beyond their original fixed-length input setting. Without full retraining, we introduced a lightweight plug-in adaptation module that enables one-time extension to longer and variable-length recordings. Across multiple tasks, datasets, and backbone families, the proposed method achieves consistently strong performance, improving over snapshot aggregation baselines and remaining competitive across diverse adaptation strategies.

A key feature of the proposed method is that the extension module is trained at the longest available horizon and then evaluated across a range of different input lengths. The resulting performance indicates that the adapted models can generalize effectively across variable-duration inputs. However, extending snapshot foundation models to arbitrary or substantially longer horizons under practical memory and computational constraints remains an open challenge. We view more inference-efficient mechanisms for longer-horizon adaptation as an important direction for future work.

Table 3: **Ablation of adaptation components for CSFM on VTaC (AUC %).**

PE Strategy	$\mathcal{L}_{\text{local}}$	$\mathcal{L}_{\text{dyn}}$	10s	30s	60s	120s	180s
Repeat	✗	✗	70.43	73.09	70.60	72.43	71.45
Interpolate	✗	✗	60.78	67.44	74.37	80.86	88.18
Global	✗	✗	78.13	83.96	87.45	89.08	88.92
Global	✓	✗	83.62	87.13	88.42	89.30	89.00
Global	✗	✓	80.01	85.90	87.80	88.86	88.90
Global	✓	✓	<b>84.10</b>	<b>88.29</b>	<b>89.01</b>	<b>89.76</b>	<b>89.50</b>

Table 4: **Affinity-guided dropping** compared with random dropping (AUC %).

Model	Strategy	10s	30s	60s	120s	180s
CSFM-Tiny	Affinity Drop	<b>84.10</b>	<b>88.29</b>	<b>89.01</b>	89.76	<b>89.50</b>
	Random Drop	84.00	87.19	88.35	<b>90.03</b>	89.01
CSFM-Base	Affinity Drop	<b>87.38</b>	<b>89.15</b>	<b>89.50</b>	<b>90.85</b>	<b>91.23</b>
	Random Drop	86.73	88.01	88.93	90.16	90.83
ECG-JEPA	Affinity Drop	<b>78.86</b>	<b>82.93</b>	<b>86.09</b>	<b>89.36</b>	<b>91.02</b>
	Random Drop	75.92	80.79	84.87	88.92	90.01
MERL	Affinity Drop	<b>61.23</b>	<b>76.03</b>	<b>80.27</b>	<b>83.68</b>	<b>82.60</b>
	Random Drop	58.20	72.54	78.67	80.23	81.20

## References

- [1] Konstantinos C Siontis, Peter A Noseworthy, Zachi I Attia, and Paul A Friedman. Artificial intelligence-enhanced electrocardiography in cardiovascular disease management. *Nature Reviews Cardiology*, 18(7):465–478, 2021.
- [2] Nils Strodthoff, Patrick Wagner, Tobias Schaeffter, and Wojciech Samek. Deep learning for ecg analysis: Benchmarks and insights from ptb-xl. *IEEE journal of biomedical and health informatics*, 25(5):1519–1528, 2020.
- [3] Jun Li, Aaron Aguirre, Junior Moura, Che Liu, Lanhai Zhong, Chenxi Sun, Gari Clifford, Brandon Westover, and Shenda Hong. An electrocardiogram foundation model built on over 10 million recordings with external evaluation across multiple domains. *arXiv preprint arXiv:2410.04133*, 2024.
- [4] Xiao Gu, Yuxuan Shu, Jinpei Han, Yuxuan Liu, Zhangdaihong Liu, James Anibal, Veer Sangha, Edward Phillips, Bradley Segal, Yuxuan Liu, Hang Yuan, Fenglin Liu, Kim Branson, Patrick Schwab, Danielle Belgrave, Lei Clifton, Dimitris Spathis, Vasileios Lampos, A. Aldo Faisal, and David A. Clifton. Foundation models for biosignals: A survey. 2025.
- [5] Kaden McKeen, Sameer Masood, Augustin Toma, Barry Rubin, and Bo Wang. Ecg-fm: An open electrocardiogram foundation model. *JAMIA open*, 8(5):ooaf122, 2025.
- [6] Xiao Gu, Wei Tang, Jinpei Han, Veer Sangha, Fenglin Liu, Shreyank N Gowda, Antonio H Ribeiro, Patrick Schwab, Kim Branson, Lei Clifton, et al. Cardiac health assessment across scenarios and devices using a multimodal foundation model pretrained on data from 1.7 million individuals. *Nature Machine Intelligence*, 8(2):220–233, 2026.
- [7] Jun Li, Aaron D Aguirre, Valdery Moura Junior, Jiarui Jin, Che Liu, Lanhai Zhong, Chenxi Sun, Gari Clifford, M Brandon Westover, and Shenda Hong. An electrocardiogram foundation model built on over 10 million recordings. *NEJM AI*, 2(7):AIoa2401033, 2025.
- [8] Li-wei Lehman, Benjamin Moody, Harsh Deep, Feng Wu, Hasan Saeed, Lucas McCullum, Diane Perry, Tristan Struja, Qiao Li, Gari Clifford, and Roger Mark. VTaC: A benchmark dataset of ventricular tachycardia alarms from ICU monitors. In *Advances in Neural Information Processing Systems (NeurIPS)*, pages 38827–38843, 2023.
- [9] Benjamin Moody, George Moody, Mauricio Villarroel, Gari D. Clifford, and Ikaro Silva. MIMIC-III Waveform Database Matched Subset. *PhysioNet*, April 2020. doi: 10.13026/c2294b. URL <https://doi.org/10.13026/c2294b>. Version 1.0.
- [10] Aman Kansal, Emma Chen, Boyang Tom Jin, Pranav Rajpurkar, and David A Kim. MC-MED, multimodal clinical monitoring in the emergency department. *Scientific Data*, 12(1):1094, 2025.
- [11] Zhijiang Wan, Qianhao Yu, Jia Mao, Wenfeng Duan, and Cheng Ding. Openecg: Benchmarking ecg foundation models with public 1.2 million records. *arXiv preprint arXiv:2503.00711*, 2025.
- [12] Jonathan B Moody, Alexis Poitrasson-Rivière, Jennifer M Renaud, Tomoe Hagio, Fares Alahdab, Mouaz H Al-Mallah, Michael D Vanderver, Sascha N Goonewardena, Edward P Ficaró, and Venkatesh L Murthy. A foundation transformer model with self-supervised learning for ecg-based assessment of cardiac and coronary function. *NEJM AI*, 2(12):AIoa2500164, 2025.
- [13] Junho Song, Jong-Hwan Jang, DongGyun Hong, Joon myoung Kwon, and Yong-Yeon Jo. Crema: A contrastive regularized masked autoencoder for robust ecg diagnostics across clinical domains, 2025. URL <https://arxiv.org/abs/2407.07110>.
- [14] Shaoting Zhang, Yishan Du, Wenji Wang, Xianying He, Fangfang Cui, Liang Zhao, Bei Wang, Zhiqiang Hu, Ziqiang Wang, Qing Xia, et al. Ecgfm: A foundation model for ecg analysis trained on a multi-center million-ecg dataset. *Information Fusion*, page 103363, 2025.
- [15] Han Yu, Peikun Guo, and Akane Sano. Ecg semantic integrator (esi): A foundation ecg model pretrained with llm-enhanced cardiological text. *Transactions on Machine Learning Research (TMLR)*, 2024.

- [16] Yuanyuan Tian, Zhiyuan Li, Yanrui Jin, Mengxiao Wang, Xiaoyang Wei, Liqun Zhao, Yunqing Liu, Jinlei Liu, and Chengliang Liu. Foundation model of ecg diagnosis: Diagnostics and explanations of any form and rhythm on ecg. *Cell Reports Medicine*, 5(12), 2024.
- [17] Wei-Long Zheng, Edilberto Amorim, Jin Jing, Wendong Ge, Shenda Hong, Ona Wu, Mohammad Ghassemi, Jong Woo Lee, Adithya Sivaraju, Trudy Pang, et al. Predicting neurological outcome in comatose patients after cardiac arrest with multiscale deep neural networks. *Resuscitation*, 169:86–94, 2021.
- [18] Peng Zhang, Fan Lin, Fei Ma, Yuting Chen, Siyi Fang, Haiyan Zheng, Zuwen Xiang, Xiaoyun Yang, and Qiang Li. Automatic screening of patients with atrial fibrillation from 24-h holter recording using deep learning. *European Heart Journal-Digital Health*, 4(3):216–224, 2023.
- [19] Suli Wang, Yangshen Deng, Zhenghua Bao, Xinyu Zhan, and Yiqun Duan. Neurottt: Bridging pretraining-downstream task misalignment in eeg foundation models via test-time training. *arXiv preprint arXiv:2509.26301*, 2025.
- [20] Rushuang Zhou, Yuanting Zhang, and Yining Dong. H-tuning: Toward low-cost and efficient ECG-based cardiovascular disease detection with pre-trained models. In *Forty-second International Conference on Machine Learning*, 2025. URL <https://openreview.net/forum?id=RLu1QIPiVr>.
- [21] Chenrui Wu, Haishuai Wang, Xiang Zhang, Chengqi Zhang, and Jiajun Bu. Efficient personalized adaptation for physiological signal foundation model. In *Forty-second International Conference on Machine Learning*, 2025. URL <https://openreview.net/forum?id=55ysNwb0TI>.
- [22] Alexey Dosovitskiy, Lucas Beyer, Alexander Kolesnikov, Dirk Weissenborn, Xiaohua Zhai, Thomas Unterthiner, Mostafa Dehghani, Matthias Minderer, Georg Heigold, Sylvain Gelly, Jakob Uszkoreit, and Neil Houlsby. An image is worth 16x16 words: Transformers for image recognition at scale. In *International Conference on Learning Representations*, 2021. URL <https://openreview.net/forum?id=YicbFdNTTy>.
- [23] Hangbo Bao, Li Dong, Songhao Piao, and Furu Wei. BEit: BERT pre-training of image transformers. In *International Conference on Learning Representations*, 2022. URL <https://openreview.net/forum?id=p-BhZSz59o4>.
- [24] Ze Liu, Yutong Lin, Yue Cao, Han Hu, Yixuan Wei, Zheng Zhang, Stephen Lin, and Baining Guo. Swin transformer: Hierarchical vision transformer using shifted windows. In *Proceedings of the IEEE/CVF International Conference on Computer Vision (ICCV)*, 2021.
- [25] Menglin Jia, Luming Tang, Bor-Chun Chen, Claire Cardie, Serge Belongie, Bharath Hariharan, and Ser-Nam Lim. Visual prompt tuning. In *European Conference on Computer Vision (ECCV)*, pages 709–727, 2022.
- [26] Seunghan Lee, Taeyoung Park, and Kibok Lee. Soft contrastive learning for time series. In *12th International Conference on Learning Representations, ICLR 2024*, 2024.
- [27] Dani Kiyasseh, Tingting Zhu, and David A Clifton. Clocs: Contrastive learning of cardiac signals across space, time, and patients. In *International Conference on Machine Learning*, pages 5606–5615. PMLR, 2021.
- [28] Kaiwen Zha, Peng Cao, Jeany Son, Yuzhe Yang, and Dina Katabi. Rank-n-contrast: learning continuous representations for regression. *Advances in Neural Information Processing Systems*, 36:17882–17903, 2023.
- [29] Ting Chen, Simon Kornblith, Mohammad Norouzi, and Geoffrey Hinton. A simple framework for contrastive learning of visual representations. In *International conference on machine learning*, pages 1597–1607. PmlR, 2020.
- [30] Xinlei Chen and Kaiming He. Exploring simple siamese representation learning. In *Proceedings of the IEEE/CVF conference on computer vision and pattern recognition*, pages 15750–15758, 2021.

- [31] Chaoqi Yang, M Westover, and Jimeng Sun. Biot: Biosignal transformer for cross-data learning in the wild. *Advances in Neural Information Processing Systems*, 36:78240–78260, 2023.
- [32] Che Liu, Zhongwei Wan, Cheng Ouyang, Anand Shah, Wenjia Bai, and Rossella Arcucci. Zero-shot ECG classification with multimodal learning and test-time clinical knowledge enhancement. In *International Conference on Machine Learning (ICML)*, pages 31949–31963, 2024.
- [33] Sehun Kim. Learning general representation of 12-lead electrocardiogram with a joint-embedding predictive architecture, 2026. URL <https://arxiv.org/abs/2410.08559>.
- [34] Li-wei Lehman, Benjamin Moody, Lucas McCullum, Hasan Saeed, Harsh Deep, Diane Perry, Tristan Struja, Qiao Li, Gari Clifford, and Roger Mark. VTaC: A benchmark dataset of ventricular tachycardia alarms from ICU monitors. *PhysioNet*, October 2024. doi: 10.13026/8td2-g363. URL <https://doi.org/10.13026/8td2-g363>. Version 1.0.
- [35] Aman Kansal, Emma Chen, Tom Jin, Pranav Rajpurkar, and David Kim. Multimodal Clinical Monitoring in the Emergency Department (MC-MED). *PhysioNet*, September 2025. doi: 10.13026/wvyw-g663. URL <https://doi.org/10.13026/wvyw-g663>. Version 1.0.1.
- [36] Xingyao Wang, Caiyun Ma, Xiangyu Zhang, Hongxiang Gao, Gari D. Clifford, and Chengyu Liu. Paroxysmal Atrial Fibrillation Events Detection from Dynamic ECG Recordings: The 4th China Physiological Signal Challenge 2021. *PhysioNet*, June 2021. doi: 10.13026/ksya-qw89. URL <https://doi.org/10.13026/ksya-qw89>. Version 1.0.0.
- [37] Shoufa Chen, Chongjian Ge, Zhan Tong, Jiangliu Wang, Yibing Song, Jue Wang, and Ping Luo. AdaptFormer: Adapting vision transformers for scalable visual recognition. *Advances in Neural Information Processing Systems (NeurIPS)*, 35:16664–16678, 2022.
- [38] Jonas Pfeiffer, Aishwarya Kamath, Andreas Rücklé, Kyunghyun Cho, and Iryna Gurevych. AdapterFusion: Non-destructive task composition for transfer learning. In *Proceedings of the 16th conference of the European chapter of the association for computational linguistics*, pages 487–503, 2021.